Journal of Molecular Structure 1270 (2022) 133946

Contents lists available at ScienceDirect

Journal of Molecular Structure

journal homepage: www.elsevier.com/locate/molstr

Benzimidazole-hydrazone derivatives: Synthesis, *in vitro* anticancer, antimicrobial, antioxidant activities, *in silico* DFT and ADMET studies

Ayşen IŞIK[a], Ulviye Acar Çevik[b,*], Ismail Çelik[c], Hayrani Eren Bostancı[d], Arzu Karayel[e], Gülsüm Gündoğdu[f], Ufuk Ince[g], Ahmet Koçak[h], Yusuf Özkay[b], Zafer Asım Kaplancıklı[b]

[a] Department of Biochemistry, Faculty of Science, Selçuk University, Konya, Turkey
[b] Department of Pharmaceutical Chemistry, Faculty of Pharmacy, Anadolu University, Eskişehir 26470, Turkey
[c] Department of Pharmaceutical Chemistry, Faculty of Pharmacy, Erciyes University, Kayseri 38039, Turkey
[d] Department of Biochemistry, Faculty of Pharmacy, Cumhuriyet University, Sivas, Turkey
[e] Department of Physics, Faculty of Arts and Science, Hitit University, Çorum 19030, Turkey
[f] Department of Energy Science and Technology, Faculty of Science, Turkish-German University, Istanbul 34820, Turkey
[g] Department of Pharmaceutical Microbiology, Faculty of Pharmacy, Erciyes University, Kayseri 38039, Turkey
[h] Department of Chemistry, Faculty of Science, Selçuk University, Konya, Turkey

ARTICLE INFO

Article history:
Received 16 February 2022
Revised 17 July 2022
Accepted 13 August 2022
Available online 14 August 2022

Keywords:
Benzimidazole
Anticancer
Antimicrobial
Antioxidant
DFT
ADMET
PXRD

ABSTRACT

Based on the biologically active heterocycle compounds, a series of new benzimidazole-hydrazone derivatives (**3a-3j**) were synthesized, starting from 4-(6-chloro-1*H*-benzimidazol-2-yl) benzohydrazide. The synthesized compounds were characterized by ^{1}H NMR, ^{13}C NMR, and HRMS spectroscopic methods. The synthesized compounds were preliminarily evaluated for their *in vitro* antimicrobial, anticancer and antioxidant activity. The antimicrobial activity was checked against *S. aureus* ATCC 29213, *E. coli* ATCC 25922, and *C. albicans* ATCC 10231 by micro-dilution method. The findings exhibited that the compounds possessed moderate antimicrobial potential. The compounds were also checked for their *in vitro* anticancer activities against HT-29 (colorectal cancer cell line) using the MTT assay. It was observed that all the compounds **3a-3j** showed weak antiproliferative activity against HT-29 cells. The compounds were also analyzed for their antioxidant capacity by Tas & Tos activity. The compound **3d** showed a high antioxidative effect with 30.81 µmol H_2O_2 Equiv./L value. The lowest energy state of compound **3d** was realized in DMSO medium by using the B3LYP method at 6–311G (d,p) level, the optimized geometry of it is about 0.50 and 17 kcal/ mol more stable than in other solvents and the gas phase, respectively. The lower ΔE=3.563 eV indicates the higher reactivity of compound **3d**, this is compatible with biological experimental data and shows high antioxidant property of the compound. *In silico* ADMET studies of compound **3d** were performed. Indexing of the X-ray powder diffraction pattern was performed for compound **3a**.

1. Introduction

Cancer is one of the deadliest diseases. The disease, which starts with uncontrolled cell growth, causes metastasis by spreading to surrounding tissues. Metastasis becomes a main cause of death when cancer treatment fails [1]. In the world cancer report published by WHO, it is reported that the rate of death due to cancer will nearly double in the coming years [2]. Today, the biggest obstacle in therapeutic cancer treatment is that anticancer drugs are also toxic to normal cells and this causes many side effects [3]. This situation limits the effectiveness of the current treatment. Therefore, there is a great need for the discovery of new and potent chemotherapeutics with minimal side effects in the development of new treatment approaches.

Considering the needs of developing/developed countries, antibacterial drugs have emerged, and their usage rates have increased especially recently. Although the worldwide prevalence of antimicrobial resistance as a result of overuse and misuse of antimicrobial drugs has reduced the effectiveness of existing treatment methods. This has also made a significant contribution to the development of new antimicrobial agents [4]. The development of new and effective antimicrobial agents is of great importance to prevent the further spread of drug resistance.

Based on the above developments, we can say that the development of new, effective antimicrobial and anticancer therapeutic agents has critical importance in medicinal chemistry. In the studies carried out so far, it has been accepted that heterocyclic com-

* Corresponding author.
E-mail address: uacar@anadolu.edu.tr (U. Acar Çevik).

https://doi.org/10.1016/j.molstruc.2022.133946
0022-2860/

pounds play an important role in the human biological system, and at the same time, heterocyclic compounds with a wide range of biological activities such as antimicrobial, antibiotic, antivirus and in anticancer studies have taken place in the pharmaceutical industry [5]. Therefore, the design, synthesis, and activity studies of this class of compounds have become a very attractive field for researchers.

Antioxidants protect organisms and cells from the harmful effects of oxidative stress during metabolism. The oxidation reaction transfers electrons from a material to an oxidizing agent, resulting in the formation of free radicals that harm the cells [6]. However, most of the cells comprise a complex network of antioxidant metabolites and enzymes that work together to protect cellular components, including DNA, proteins, and lipids from oxidative damage. Antioxidants are molecules that destroy free radicals, which may harm cells and tissues in organisms, as well as prevent the oxidation processes, which occur during chemical processes in metabolic pathways [7]. Thus, the antioxidant properties of synthetic substances are being explored extensively. An important research field is the quest for active chemicals that can prevent or lessen the effects of oxidative stress on cells. Moreover, free radical oxidative processes are known to have a substantial detrimental role in the development of many human diseases, as well as aging [8,9].

Benzimidazoles are an important member of the heterocyclic compound class. Benzimidazoles exhibit antitumor, antiproliferative, anticancer [10–16], antimicrobial including anti-HIV [17–21], and antioxidant activity [22,23]. Furthermore, because of its biological properties, schiff base (–C=N–) is a widely used organic ligand [24].

In this context, we aimed to synthesize new substituted derivatives containing benzimidazole and hydrazone groups based on the above information and to investigate their antimicrobial, anticancer, and antioxidant activities. In this study, we focused on the synthesis, characterization, and *in vitro* evaluation of ten different derivatives carrying benzimidazole and hydrazone moieties that are believed to have antibacterial, antifungal, anticancer, and antioxidant activities. Density Functional Theory (DFT) is a useful tool in determining the correct molecular structure essential for structure-activity relationship. For this purpose, the mentioned newly synthesized ten compounds were modeled with DFT by using conventional hybrid functional (B3LYP) [25] and by taking into account long-range interaction (wB97X-D) [26]. Both van der Waals and solvent effect on the molecular structure were investigated. HOMO-LUMO analysis has been used to shed light on the information about charge transfer within the molecule. In addition, computational ADMET analysis of compound **3d** with the highest antioxidant activity was performed.

2. Result and discussion

2.1. Chemistry

The synthetic routes to obtain benzimidazole-hydrazone derivatives (**3a-3j**) are shown in **Scheme 1**. The synthesis of the starting 4-(5-chloro-1*H*-benzimidazol-2-yl) benzoic acid methyl ester (1) was accomplished by refluxing 5-chloro-1,2-phenylenediamine and 4-formylbenzoic acid methyl ester sodium disulfide salt according to the procedure described by us earlier [27]. In the second step, compound **1** was substituted with hydrazine hydrate, resulting in the corresponding acetohydrazide (2). Condensation of 4-(5-chloro-1*H*-benzimidazol-2-yl) benzoic acid hydrazide (2) with different aldehydes yielded a series of *N*-acylhydrazones (**3a-3j**). The structures of all compounds (**Scheme 1**) were determined with the help of different spectroscopic techniques such as ^{1}H NMR, ^{13}C NMR, and HRMS.

Table 1
In vitro MICs (μg/mL) observed of the compounds (**3a-3j**) and reference antimicrobial drugs.

Compounds	Microorganisms					
	S. a.	S. a. *	E. c.	E. c. *	C. a.	C. a.*
3a	256	256	256	256	256	256
3b	256	256	256	128	256	256
3c	256	256	256	128	256	256
3d	256	256	128	128	256	256
3e	256	256	128	256	256	256
3f	128	256	256	256	256	256
3g	256	256	256	256	256	256
3h	256	256	256	128	256	256
3ı	256	256	128	128	256	256
3j	256	256	256	256	128	256
Ampicilin	2	32	16	16	-	-
Gentamycin	1	8	1	16	-	-
Vancomycin	1	4	-	-	-	-
Fluconazole	-	-	-	-	1	1

S.a.: *Staphylococcus aureus* ATCC 29213; S.a.*: *S. aureus* isolate (MRSA); E.c.: *E. coli* ATCC 25922; E.c.*: *E. coli* isolate (contains broad spectrum β-lactamase enzyme -GSBL-); C.a: *Candida albicans* ATCC 10231; C. a.*: *Candida albicans* isolate

In the ^{1}H NMR spectra of **3a**-**3f,** the signals for the protons of the azomethine group were found at 8.42–9.24 ppm as singlets. The benzimidazole protons produced multiplet signals within the interval 7.26–7.72 ppm in DMSO solvent, while the phenyl protons resonated in the interval 6.70–8.33 ppm. The chemical shift values for the protons for the NH protons varied in a broader range of 11.65–13.33 ppm.

2.2. Biological activity evaluation

2.2.1. Antimicrobial activity

The minimum inhibitory concentration (MIC) values were determined for each substance and reference antimicrobial agent shown in **Table 1**. The MIC values of the compounds were compared to reference antimicrobials (Ampicillin, gentamicin and vancomycin for antibacterial, fluconazole for antifungal activity). According to the result of the study, the compound with the best MIC value on the *S. aureus* ATCC 29213 strain was compound **3f** with 128 µg/mL. All compounds had MIC value of 256 µg/mL on the clinical isolate of *S. aureus* and MIC values in the 128–256 µg/mL range on the *E. coli* ATCC 25922 strain and its clinical isolate.

The compound with the best antifungal activity was compound **3j** which had MIC value of 128 µg/mL on *C. albicans* ATCC 10231. The results show that the compounds in our study did not reach the MIC values of the reference antimicrobials and had moderate levels of antimicrobial activity.

2.2.2. Anticancer activity

Anticancer activity of compounds **3a-3j** was evaluated against the HT-29 cell line. For preliminary screening, cytotoxic bioactivity of synthesized compounds was evaluated *in vitro* against the HT-29 cell line with the MTT assay. To evaluate the anticancer potency of target compounds, the cancer cells were treated with the compounds at 20 μM constant concentration. Cell viability percentages were calculated after the treatment of cells for 24 h. Fluorouracil was used as a positive control. Preliminary anticancer activity results of compounds **3a-3j** against HT-29 are presented in **Table 2**. It was observed that some of compounds **3a-3j** showed weak antiproliferative activity against HT-29 cells. However, when compared with the positive control, it was determined that the studied compounds did not show considerable anticancer properties.

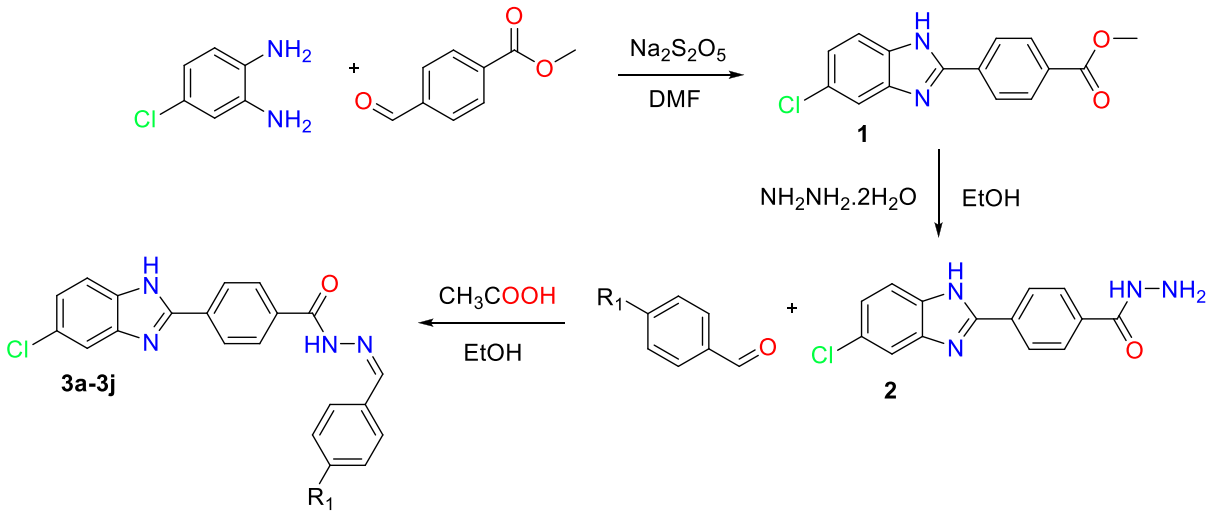

Comp.	R_1
3a	-COOH
3b	-*N*,*N*-diethylamine
3c	-isopropyl
3d	-methylthio
3e	- trifluoromethyl
3f	-phenyl
3g	-ethoxy
3h	-benzyloxy
3i	-cyano
3j	-*o*-COOH

Scheme 1. General procedure for synthesis of the final compounds **3a-3j.**

Table 2
After 24 h % viability of HT-29 cell line.

Compound	24h Viability %
3a	79.2 ± 6.28
3b	72.8 ± 9.56
3c	75.6 ± 7.14
3d	79.3 ± 6.83
3e	74.2 ± 10.61
3f	75.3 ± 6.74
3g	79.5 ± 4.21
3h	75.6 ± 4.69
3ı	89.6 ± 4.10
3j	91.9 ± 7.00
Fluorourasil	22.1 ± 4.84

Table 3
Total Antioxidan Status (TAS) and Total oxidative Status (TOS) values.

Compound	TAS mmol Trolox equiv./L	TOS µmol H_2O_2 Equiv./L
3a	0.003 ± 0.001	18.26 ± 0.42
3b	0.029 ± 0.007	19.13 ± 0.27
3c	0.003 ± 0.001	19.80 ± 1.09
3d	**1.370 ± 0.058**	**30.81 ± 0.84**
3e	0.013 ± 0.005	19.40 ± 1.13
3f	0.013 ± 0.003	18.86 ± 0.93
3g	0.072 ± 0.009	18.99 ± 0.87
3h	0.322 ± 0.019	18.39 ± 1.56
3ı	0.019 ± 0.004	19.13 ± 2.09
3j	0.104 ± 0.007	19.73 ± 0.49

2.2.3. Antioxidant activity

The total antioxidant capacity values greater than or equal to 1.0 mmol Trolox Equiv./L are considered as high. Total antioxidant capacity values of the compounds between **3a-3j** were found low except **3d** which is shown in **Table 3.** Compound **3d** was found to have more antioxidant capacity than 1 mmol Vitamin E. However, a structure that is expected to show anticancer properties should have oxidative properties. The oxidative effects of structures with the activity of 20 µmol H_2O_2 Equiv./L and above are considered strong. As seen in **Table 3**, it was determined that the compound **3d** showed a high oxidative effect with 30.81 µmol H_2O_2 Equiv./L value. When compound **3d** was examined, it was found that the presence of a methylthio group in the para position of the phenyl ring attached to the hydrazone structure increased the antioxidant activity. However, despite these properties, the compound **3d** could

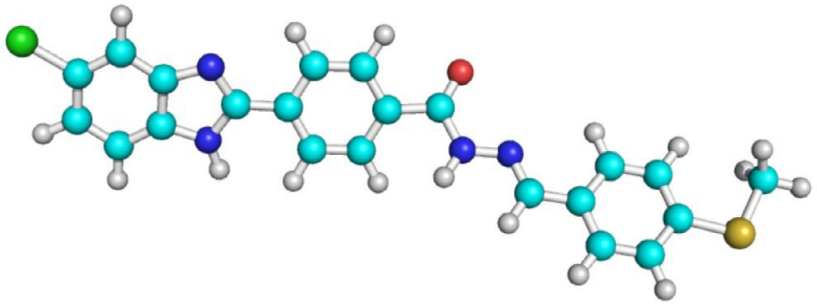

Fig. 1. The optimized geometry of **3d** in gase phase at B3LYP/6-311G(d,p) level.

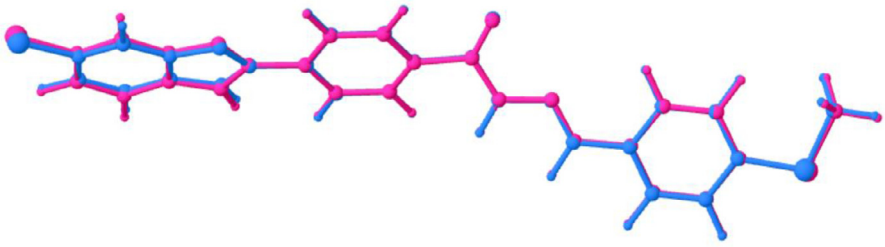

Fig. 2. Superposition of the geometries of 3d in DMSO medium by using B3LYP (pink) and wB97X-D (blue) at 6-311G(d,p) level with RMSD value of 0.097 Å.

not show the desired anticancer properties. Though, it can be used as a potential cancer inhibitor in different cancer cell lines.

2.3. Computational studies

2.3.1. Density Functional Theory (DFT) calculations

Density functional theory is a functional tool in determining the correct molecular structure that corresponds to the lowest energy state at the potential energy surface. In the structure-activity relationship, it is essential to determine the accurate structure. For this purpose, the newly synthesized ten compounds are modeled with Density Functional Theory (DFT) by using conventional hybrid functional (B3LYP) [25] and by taking into account long-range interaction (wB97X-D) [26].

All structures have no imaginary frequencies; this state indicates that they are being at global ninima on potential energy surface. The optimization results of molecule **3d** indicate that the rotations of the chloro-benzimidazole group with respect to the benzo-hydrazine group are 173.12° for B3LYP and 167.17° for wB97X-D functional in DMSO medium, while the rotations of methylthio-benzylidene group relative to the benzo-hydrazine group are 179.95° and -178.90°, respectively. The optimized geometries in DMSO correspond to the lowest energy geometry between the gas phase and other solvent mediums. The optimized geometry of **3d** in gas phase is shown in **Fig. 1**.

The root-mean-square deviation (RMSD) of optimized structure (B3LYP) is 0.097 Å with wB97X-D functional, indicating the good harmony between two optimized structures, as shown in **Fig. 2**. While the geometries are quite compatible according to superposition, the energies are quite different from each other. The optimized energy for B3LYP is the lowest in the DMSO medium, that energy is smaller about 0.5 kcal/mol and 17 kcal/mol than that of other solvent mediums and gas phase, respectively. The wB97X-D also complied with the same trend.

HOMO-LUMO and molecular electrostatic potential (MEP) diagrams are shown in **Fig. 3**. HOMO-LUMO analysis is showing that the charge in HOMO is localized on methylthio benzylidene and hydrazine group, while the orbital lobs in LUMO are localized throughout the molecule except for methyl.

Electrophilic and nucleophilic reactive regions of the molecule can be identified with the help of the MEP map. According to this MEP (**Fig. 3**), the hydrogen lınked to nitrogen atom existing in imidazole ring and the hydrogen of nitrogen atom existing in benzo hydrazine group have the highest positive potential (blue sites), which is managing nucleophilic attack. In addition, the oxygen atom existing in the benzo hydrazine group and the nitrogen atom of the imidazole ring possess the highest negative potential (red cites), responsible for the electrophilic attack.

The lower energy gap means chemically more reactive. According to **Tables 4**, **3b** and **d** molecules are chemically more reactive than the other molecules. The chemical reactivity order is that 3b>3d>3g>3h>3f>3e>3a>3i>3j>3c.

2.3.2. ADMET prediction

As given in **Table 5**, the solubility of most antioxidant active compound **3d** in water is low, $CaCO_2$ permeability reference value Papp $> 8 \times 10^{-6}$ cm/s is suitable, an *in vitro* model of the human intestinal mucosa. Human intestinal absorption is good and skin permeability is low. P-glycoprotein acts as a biological barrier, removing toxins and xenobiotics from cells. Compound **3d** exhibits P-glycoprotein I and II inhibitory properties. The steady-state volume of distribution (VDss) is low, the fraction of unbounded drug is low, and it largely bounds to blood plasma proteins. It has weak BBB permeability and can penetrate CNS. It has the potential to inhibit CYP enzymes, so it can interact with other drug molecules. Drug clearance occurs as a combination of hepatic clearance and renal clearance. The total clearance of compound **3d** is 0.867. It has the property of being a renal Organic Cation Transporter 2 (OCT2) substrate, which is a contraindication for drugs used as OCT2 inhibitors. Compound **3d** may exhibit AMES toxicity, meaning it may be mutagenic. The maximum recommended tolerated dose is low, that is, below 0.477 log (mg/kg/day). Inhibition of the potassium channels encoded by hERG is the principal cause for the development of fatal ventricular arrhythmia. Compound **3d** has no hERG I

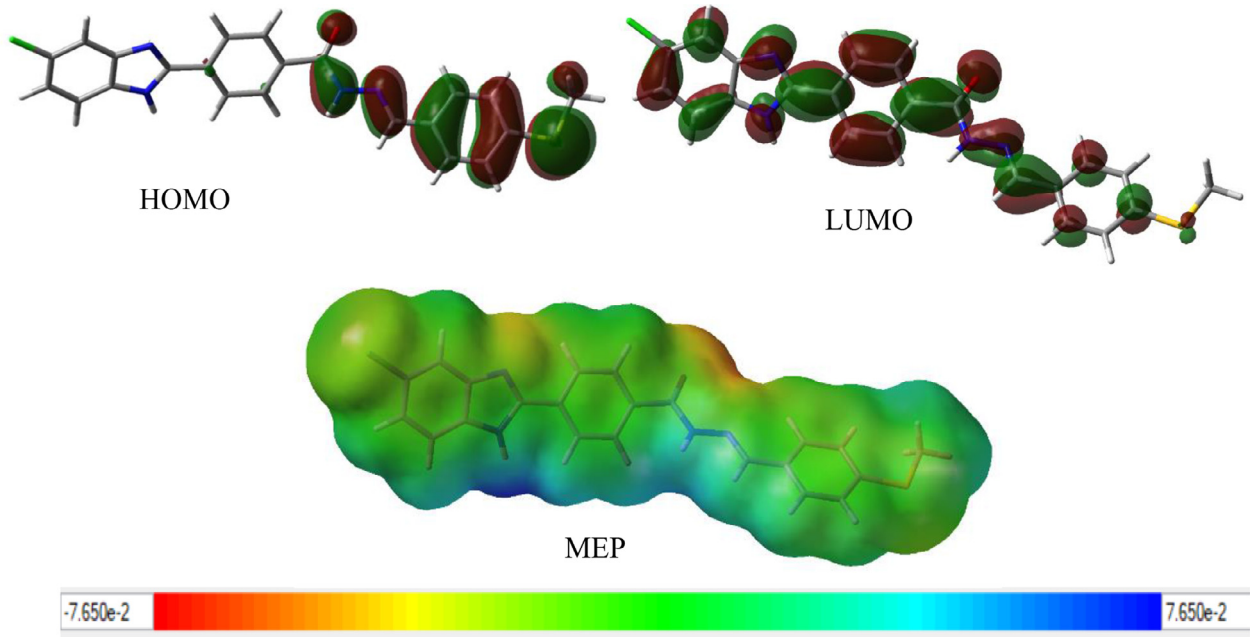

Fig. 3. HOMO-LUMO and MEP diagrams of 3d at B3LYP/6-311G(d,p) level.

Table 4
HOMO-LUMO energies (eV) and calculated global reactivity parameters of **3a**-**3j** at B3LYP/6-311G(d,p) level in gas phase.

Comp.	LUMO	HOMO	ΔE(eV)	IP(eV)	EA(eV)	X(eV)	η(eV)	S(eV)$^{-1}$	μ(eV)	ω(eV)
3a	-2.523	-6.408	3.884	6.408	2.523	4.466	1.942	0.257	-4.466	5.134
3b	-2.068	-5.292	3.224	5.292	2.068	3.680	1.612	0.310	-3.680	4.200
3c	-2.128	-6.170	4.042	6.170	2.128	4.149	2.021	0.247	-4.149	4.259
3d	-2.240	-5.803	3.563	5.803	2.240	4.022	1.782	0.281	-4.022	4.539
3e	-2.654	-6.465	3.811	6.465	2.654	4.559	1.905	0.262	-4.559	5.455
3f	-2.041	-5.842	3.801	5.842	2.041	3.941	1.900	0.263	3.941	4.087
3g	-2.169	-5.867	3.698	5.867	2.169	4.018	1.849	0.270	-4.018	4.366
3h	-2.168	-5.869	3.701	5.869	2.168	4.019	1.850	0.270	-4.019	4.365
3i	-2.404	-6.311	3.907	6.311	2.404	4.358	1.954	0.256	-4.358	4.860
3j	-2.422	-6.404	3.983	6.404	2.422	4.413	1.991	0.251	-4.413	4.890

Gap ΔE: (E_{LUMO}-E_{HOMO}), IP **(-HOMO):** Ionization potential, EA **(-LUMO)**: Electron affinity, X **(*IP*+*EA*)/2**: Electronegativity, η **(IP−EA)/2**: Chemical hardness, S (**1/2η**): chemical softness, μ **−(IP+EA)/2**: Chemical potential, ω **(μ^2 /2η)**: Electrophilic index.

inhibitory property, while inhibits hERG II. Oral Rat Acute Toxicity (LD_{50}) and Oral Rat Chronic Toxicity (LOAEL) values were found to be 2.479 mol/kg and 1.548 log mg/kg_bw/day respectively. It may show hepatotoxicity, but not the skin sensitization. *T.Pyriformis* toxicity is 0.285, the value > -0.5 log ug/L is considered toxic. Since the lethal concentration value is below 0.5, it may show high acute toxicity.

2.4. PXRD data analysis

Indexing of the X-ray powder diffraction pattern was carried out using the TOPAS Academic program v5.1 [44], yielding the following values for triclinic space group $P1^-$ of the compound **3a**: a = 10.857 Å, b = 9.777 Å, c = 12.980 Å, α = 92.68°, β = 88.10°, γ = 84.83°, V = 1369.92 Å3. Then Pawley refinement for the whole powder pattern of the compound was performed to confirm the choice of space group as well as unit cell parameters. The values of unit cell parameters as well as R-factors and goodness-of-fit indicator found after refinement were of compound **3a**: a = 11.028(7) Å, b = 9.822(8) Å, c = 13.050(8) Å, α = 92.224(38) °, β = 88.204(41)°, γ = 84.981(48) ° and V = 1406(1) Å3, Rwp= 6.970%, Rexp= 4.121% and χ2 = 1.691 resulting in a good visual fit of the whole pattern (**Fig. 4**).

3. Material and methods

3.1. Experimental

Whole chemicals employed in the synthetic procedure were purchased from Sigma-Aldrich Chemicals (Sigma-Aldrich Corp., St. Louis, MO, USA) or Merck Chemicals (Merck KGaA, Darmstadt, Germany). Melting points of the obtained compounds were determined by the MP90 digital melting point apparatus (Mettler Toledo, OH, USA) and were uncorrected. ^{1}H NMR and ^{13}C NMR spectra of the synthesized compounds were obtained by a Bruker 300 MHz and 75 MHz digital FT-NMR spectrometer (Bruker Bioscience, Billerica, MA, USA) in DMSO-d_6, respectively. Splitting patterns were designated as follows: s: singlet; d: doublet; t: triplet; m: multiplet in the NMR spectra. Coupling constants (*J*) were reported as Hertz. M+1 peaks were determined by Shimadzu LC/MS ITTOF system (Shimadzu, Tokyo, Japan). All reactions were monitored by thin-layer chromatography (TLC) using Silica Gel 60 F254 TLC plates (Merck KGaA, Darmstadt, Germany).

3.1.1. Chemistry

Synthesis of 4-(5-chloro-1H-benzimidazol-2-yl)benzoic acid methyl ester (1): In a microwave synthesis reactor (Anton-Paar Monowave

Table 5
Computational absorption, distribution, metabolism, excretion, and toxicity properties of compound **3d** having best antioxidant activity.

Property	Model Name	Predicted Value	Unit
Absorption	Water solubility	**-2.888**	Numeric (log mol/L)
	Caco2 permeability	**0.845**	Numeric (log Papp in 10^{-6} cm/s)
	Intestinal absorption (human)	**79.111**	Numeric (% Absorbed)
	Skin Permeability	**-2.735**	Numeric (log Kp)
	P-glycoprotein substrate	**Yes**	Categorical (Yes/No)
	P-glycoprotein I inhibitor	**Yes**	Categorical (Yes/No)
	P-glycoprotein II inhibitor	**Yes**	Categorical (Yes/No)
Distribution	VDss (human)	**0.307**	Numeric (log L/kg)
	Fraction unbound (human)	**0.133**	Numeric (Fu)
	BBB permeability	**-0.942**	Numeric (log BB)
	CNS permeability	**-1.703**	Numeric (log PS)
Metabolism	CYP2D6 substrate	**No**	Categorical (Yes/No)
	CYP3A4 substrate	**Yes**	Categorical (Yes/No)
	CYP1A2 inhibitor	**Yes**	Categorical (Yes/No)
	CYP2C19 inhibitor	**Yes**	Categorical (Yes/No)
	CYP2C9 inhibitor	**Yes**	Categorical (Yes/No)
	CYP2D6 inhibitor	**Yes**	Categorical (Yes/No)
	CYP3A4 inhibitor	**Yes**	Categorical (Yes/No)
Excretion	Total Clearance	**0.867**	Numeric (log ml/min/kg)
	Renal OCT2 substrate	**Yes**	Categorical (Yes/No)
Toxicity	AMES toxicity	**Yes**	Categorical (Yes/No)
	Max. tolerated dose (human)	**0.206**	Numeric (log mg/kg/day)
	hERG I inhibitor	**No**	Categorical (Yes/No)
	hERG II inhibitor	**Yes**	Categorical (Yes/No)
	Oral Rat Acute Toxicity (LD50)	**2.479**	Numeric (mol/kg)
	Oral Rat Chronic Toxicity (LOAEL)	**1.548**	Numeric (log mg/kg_bw/day)

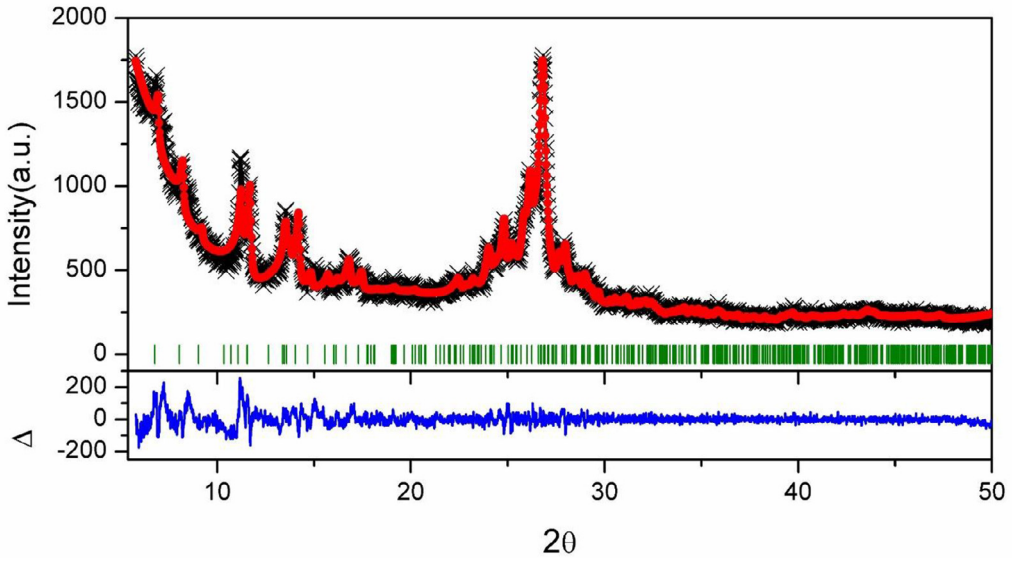

Fig. 4. Plot of the Pawley refinement of the compound **3a**. Black crosses represent observed data, the red line indicates the calculated pattern and the blue line at the bottom represents the difference between the observed and calculated patterns. Green vertical bars indicate Bragg reflections.

300) vial, 4-formylbenzoic acid methyl ester (3.2 g, 0.02 mol) and sodium metabisulfite (3.8 g, 0.02 mol) was dissolved in DMF (5 mL). The mixture was held at 240°C and 10 bar pressure for 5 min. After the mixture was cooled, 5-chloro-1,2-phenylenediamine (0.02 mol) was added and kept under the same reaction conditions. The mixture was poured into ice water, the precipitated product was filtered, washed with water, dried, and crystallized with ethanol.

Synthesis of 4-(5-chloro-1H-benzimidazol-2-yl)benzoic acid hydrazide derivatives (2): Compound **1** (0.02 mol) was dissolved in ethanol. Hydrazine hydrate (5 mL) was added to the mixture and heated in a microwave synthesis reactor (Anton-Paar Monowave 300) at 240°C and 10 bar pressure for 10 min. After cooling, the mixture was poured into ice water, the product was filtered, washed with water, and dried.

Synthesis of the final compounds (3a-3j): Appropriate 4-(5-chloro-1*H*-benzimidazol-2-yl)benzoic acid hydrazide derivative (0.001 mol) was dissolved in ethanol and aldehyde derivative (0.001 mol) with a few drops of acetic acid were added into the solution. The reaction mixture was refluxed at 100°C for 2 h. and residue was filtered, dried and recrystallized from butanol.

4-((2-(4-(5-Chloro-1*H*-benzo[*d*]imidazole-2-yl)benzoyl)hydrazineylidene)methyl)benzoic acid (**3a**); Yield: 77%, M.P.= 271.2 °C. ^{1}H-NMR (300 MHz, DMSO-d_6): δ 7.28 (1H, dd, J_1=8.55 Hz, J_2=1.98 Hz, benzimidazole-C_5), 7.65-7.72 (2H, m, benzimidazole CH), 7.88 (2H, d, J=8.28 Hz, 1,4-disubstituted benzene), 8.04 (2H, d, *J*=8.85 Hz, 1,4-disubstituted benzene), 8.13 (2H, d, J=8.31 Hz, 1,4-disubstituted benzene), 8.33 (2H, d, *J*=8.37 Hz, 1,4-disubstituted benzene), 8.55 (1H, s, CH=N), 12.17 (1H, s,

NH). ^{13}C-NMR (75 MHz, DMSO-d_6): δ= 123.29, 127.02, 127.28, 127.39, 127.64, 128.92, 130.29, 132.21, 133.09, 134.71, 136.91, 137.87, 138.76, 147.28, 152.06, 161.52, 163.05, 167.38. HRMS (m/z): $[M+H]^+$ calcd for $C_{22}H_{15}N_4O_3Cl$: 419.0919; found: 419.0905. Anal. calcd. For $C_{22}H_{15}N_4O_3Cl$, C, 63.09; H, 3.61; N, 13.38. Found: C, 63.18; H, 3.60; N, 13.41.

4-((2-(4-(5-Chloro-1*H*-benzo[*d*]imidazole-2-yl)-*N*'-(4-diethylamino)benzylidene)benzo hydrazine (**3b**); Yield: 78%, M.P.= 203.7 °C. ^{1}H-NMR (300 MHz, DMSO-d_6): δ 1.11 (6H, t, J=6.90 Hz, CH_3), 3.40-3.44 (4H, m, CH_2), 6.70 (2H, d, J=8.88 Hz, 1,4-disubstituted benzene), 7.26 (1H, s, benzimidazole CH), 7.51 (2H, d, J=8.82 Hz, 1,4-disubstituted benzene), 7.70-7.72 (2H, m, benzimidazole CH), 8.07 (2H, d, J=8.40 Hz, 1,4-disubstituted benzene), 8.28 (3H, d, J=8.40 Hz, 1,4-disubstituted benzene, CH=N), 11.65 (1H, s, NH), 13.31 (1H, s, NH). ^{13}C-NMR (75 MHz, DMSO-d_6): δ= 12.07, 13.75, 44.23, 46.04, 110.45, 112.53, 114.33, 115.16, 117.66, 120.94, 123.88, 125.87, 127.61, 128.04, 128.36, 130.41, 132.64, 135.35, 148.28, 150.56, 162.29. HRMS (m/z): $[M+H]^+$ calcd for $C_{25}H_{24}N_5OCl$: 446.1725; found: 446.1742. Anal. calcd. For $C_{25}H_{24}N_5OCl$, C, 67.33; H, 5.42; N, 15.70. Found: C, 67.45; H, 5.43; N, 15.74.

4-((2-(4-(5-Chloro-1*H*-benzo[*d*]imidazole-2-yl)-*N*'-(4-isopropylbenzylidene)benzohydrazine (**3c**); Yield: 76%, M.P.= 339.5 °C. ^{1}H-NMR (300 MHz, DMSO-d_6): δ 1.23 (6H, d, J=6.87 Hz, CH_3), 2.87-3.01 (1H, m, CH), 7.30 (1H, dd, J_1=8.58 Hz, J_2=1.98 Hz, benzimidazole-C_5), 7.36 (2H, d, J=8.19 Hz, 1,4-disubstituted benzene), 7.66-7.73 (4H, m, aromatic CH), 8.12 (2H, d, J=8.43 Hz, 1,4-disubstituted benzene), 8.33 (2H, d, J=8.43 Hz, 1,4-disubstituted benzene), 8.47 (1H, s, CH=N), 11.96 (1H, s, NH). ^{13}C-NMR (75 MHz, DMSO-d_6): δ= 24.14, 33.87, 123.50, 123.64, 127.09, 127.32, 127.44, 127.73, 128.86, 128.98, 130.74, 132.41, 132.57, 134.79, 135.17, 148.59, 151.28, 151.95, 162.77. HRMS (m/z): $[M+H]^+$ calcd for $C_{24}H_{21}N_4OCl$: 417.1482; found: 417.1477. Anal. calcd. For $C_{24}H_{21}N_4OCl$, C, 69.14; H, 5.08; N, 13.44. Found: C, 69.37; H, 5.07; N, 13.48.

4-((2-(4-(5-Chloro-1*H*-benzo[*d*]imidazole-2-yl)-*N*'-(4-(methylthio)benzylidene)benzo hydrazine (**3d**); Yield: 74%, M.P.= 316.6 °C. ^{1}H-NMR (300 MHz, DMSO-d_6): δ 2.53 (3H, s, CH_3), 7.30-7.36 (3H, m, aromatic CH), 7.67-7.70 (3H, m, aromatic CH), 7.74 (1H, s, aromatic CH), 8.12 (2H, d, J=8.40 Hz, 1,4-disubstituted benzene), 8.33 (2H, d, J=8.37 Hz, 1,4-disubstituted benzene), 8.46 (1H, s, CH=N), 11.99 (1H, s, NH). ^{13}C-NMR (75 MHz, DMSO-d_6): δ= 14.65, 115.48, 116.88, 123.76, 126.09, 127.21, 127.73, 128.04, 128.42, 128.89, 129.18, 131.09, 132.06, 135.33, 141.62, 148.20, 151.80, 162.72. HRMS (m/z): $[M+H]^+$ calcd for $C_{22}H_{17}N_4OSCl$: 421.0889; found: 421.0884. Anal. calcd. For $C_{22}H_{17}N_4OSCl$, C, 62.78; H, 4.07; N, 13.31. Found: C, 62.94; H, 4.05; N, 13.35.

4-((2-(4-(5-Chloro-1*H*-benzo[*d*]imidazole-2-yl)-*N*'-(4-(trifluoromethyl)benzylidene)benzo hydrazine (**3e**); Yield: 79%, M.P.= 260.8 °C. ^{1}H-NMR (300 MHz, DMSO-d_6): δ 7.26-7.30 (1H, m, aromatic CH), 7.59 (1H, dd, J1=8.52 Hz, J2=2.31 Hz, benzimidazole-C_5), 7.71-7.77 (1H, m, aromatic CH), 7.84 (2H, d, J=8.88 Hz, 1,4-disubstituted benzene), 7.97 (2H, d, J=7.98 Hz, 1,4-disubstituted benzene), 8.11 (2H, d, J=8.10 Hz, 1,4-disubstituted benzene), 8.32 (2H, d, J=8.49 Hz, 1,4-disubstituted benzene), 8.56 (1H, s, CH=N), 12.20 (1H, s, NH), 13.34 (1H, s, NH). ^{13}C-NMR (75 MHz, DMSO-d_6): δ= 100.68, 103.70, 107.23, 108.99, 112.73, 115.96, 120.53, 123.85, 124.79, 126.55, 126.97, 131.02, 133.52, 138.61, 142.24, 144.74, 151.39, 161.26. HRMS (m/z): $[M+H]^+$ calcd for $C_{22}H_{14}N_4OF_3Cl$: 443.0882; found: 443.0881. Anal. calcd. For $C_{22}H_{14}N_4OF_3Cl$, C, 59.67; H, 3.19; N, 12.65. Found: C, 59.85; H, 3.17; N, 12.69.

N'-([1,1'-biphenyl]-4-ylmethylene)-4-(5-chloro-1*H*-benzo[*d*]imidazole-2-yl)benzohydrazide (**3f**); Yield: 71%, M.P.= 304.1 °C. ^{1}H-NMR (300 MHz, DMSO-d_6): δ 7.28 (1H, dd, J1=8.55 Hz, J2=2.01 Hz, benzimidazole-C_5), 7.41-7.43 (1H, m, aromatic CH), 7.48-7.53 (2H, m, aromatic CH), 7.66 (2H, d, J=8.58 Hz, aromatic CH), 7.72-7.79 (3H, m, aromatic CH), 7.82-7.88 (3H, m, aromatic CH), 8.13 (2H, d, J=8.37 Hz, 1,4-disubstituted benzene), 8.33 (2H, d, J=8.40 Hz, 1,4-disubstituted benzene), 8.54 (1H, s, CH=N), 12.06 (1H, s, NH). ^{13}C-NMR (75 MHz, DMSO-d_6): δ= 123.35, 127.04, 127.16, 127.34, 127.57, 128.24, 128.38, 128.88, 129.52, 131.14, 132.84, 133.70, 133.83, 134.98, 139.77, 142.12, 148.09, 151.25, 152.06, 160.50, 162.88. HRMS (m/z): $[M+H]^+$ calcd for $C_{27}H_{19}N_4OCl$: 451.1317; found: 451.1320. Anal. calcd. For $C_{27}H_{19}N_4OCl$, C, 71.92; H, 4.25; N, 12.43. Found: C, 72.18; H, 4.23; N, 12.45.

4-((2-(4-(5-Chloro-1*H*-benzo[*d*]imidazole-2-yl)-*N*'-(4-ethoxybenzylidene)benzohydrazine (**3g**); Yield: 75%, M.P.= 279.9 °C. ^{1}H-NMR (300 MHz, DMSO-d_6): δ 1.35 (3H, t, J=6.84 Hz, CH_3), 4.08 (2H, q, J= 6.75 Hz, CH_2), 7.28 (2H, dd, J1=8.76 Hz, J2=2.10 Hz, aromatic CH), 7.26 (1H, d, J=8.52 Hz, aromatic CH), 7.63-7.70 (4H, m, aromatic CH), 8.08 (2H, d, J=8.37 Hz, 1,4-disubstituted benzene), 8.31 (2H, d, J=8.28 Hz, 1,4-disubstituted benzene), 8.42 (1H, s, CH=N), 11.86 (1H, s, NH). ^{13}C-NMR (75 MHz, DMSO-d_6): δ= 15.06, 63.73, 115.22, 123.22, 125.14, 126.16, 126.97, 127.10, 128.79, 129.26, 131.37, 132.17, 132.83, 135.10, 136.28, 148.45, 152.12, 160.68, 162.67. HRMS (m/z): $[M+H]^+$ calcd for $C_{23}H_{19}N_4O_2Cl$: 419.1253; found: 419.1269. Anal. calcd. For $C_{23}H_{19}N_4O_2Cl$, C, 65.95; H, 4.57; N, 13.38. Found: C, 66.20; H, 4.56; N, 13.41.

N'-(4-(benzyloxy)benzylidene)-4-(5-chloro-1*H*-benzo[*d*]imidazole-2-yl)benzohydrazide (**3h**); Yield: 7 0%, M.P.= 262.6 °C. ^{1}H-NMR (300 MHz, DMSO-d_6): δ 5.17 (2H, s, CH_2), 7.11 (2H, d, J=8.82 Hz, aromatic CH), 7.26 (1H, dd, J1=8.61 Hz, J2=1.92 Hz, benzimidazole-C_5), 7.34-7.44 (4H, m, aromatic CH), 7.47 (2H, d, J=8.01 Hz, aromatic CH), 7.70 (3H, d, J=8.01 Hz, aromatic CH), 8.08 (2H, d, J=8.49 Hz, 1,4-disubstituted benzene), 8.30 (2H, d, J=8.46 Hz, 1,4-disubstituted benzene), 8.42 (1H, s, CH=N), 11.87 (1H, s, NH). ^{13}C-NMR (75 MHz, DMSO-d_6): δ= 69.81, 115.66, 126.97, 127.25, 127.47, 128.27, 128.42, 128.79, 128.95, 129.24, 130.67, 131.34, 132.86, 135.08, 135.67, 137.21, 138.03, 139.48, 148.36, 148.98, 160.47, 162.69. HRMS (m/z): $[M+H]^+$ calcd for $C_{28}H_{21}N_4O_2Cl$: 481.1426; found: 481.1434. Anal. calcd. For $C_{28}H_{21}N_4O_2Cl$, C, 69.92; H, 4.40; N, 11.65. Found: C, 70.10; H, 4.39; N, 11.61.

4-((2-(4-(5-Chloro-1*H*-benzo[*d*]imidazole-2-yl)-*N*'-(4-cyanobenzylidene)benzohydrazine (**3ı**); Yield: 77%, M.P.= 285.8 °C. ^{1}H-NMR (300 MHz, DMSO-d_6): δ 7.23-7.30 (1H, m, aromatic CH), 7.58 (1H, d, J=8.61 Hz, aromatic CH), 7.70-7.77 (1H, m, aromatic CH), 7.94 (4H, s, aromatic CH), 8.11 (2H, d, J=8.25 Hz, 1,4-disubstituted benzene), 8.32 (2H, d, J=8.28 Hz, 1,4-disubstituted benzene), 8.53 (1H, s, CH=N), 12.24 (1H, s, NH), 13.33 (1H, s, NH).^{13}C-NMR (75 MHz, DMSO-d_6): δ= 111.75, 119.14, 120.82, 121.77, 122.65, 123.83, 127.03, 128.17, 128.96, 129.60, 133.28, 134.60, 134.84, 139.20, 143.12, 145.15, 146.50, 163.12. HRMS (m/z): $[M+H]^+$ calcd for $C_{22}H_{14}N_5OCl$: 400.0957; found: 400.0960. Anal. calcd. For $C_{22}H_{14}N_5OCl$, C, 66.09; H, 3.53; N, 17.52. Found: C, 65.88; H, 3.52; N, 17.56.

2-((2-(4-(5-Chloro-1*H*-benzo[*d*]imidazole-2-yl)benzoyl)hydrazineylidene)methyl)benzoic acid (**3j**); Yield: 74%, M.P.= 233.8 °C. ^{1}H-NMR (300 MHz, DMSO-d_6): δ 7.29 (1H, dd, J1=8.55 Hz, J2=1.98 Hz, benzimidazole-C_5), 7.52-7.57 (1H, m, aromatic CH), 7.65-7.72 (3H, m, aromatic CH), 7.91 (2H, d, J=7.59 Hz, aromatic CH), 8.09-8.16 (3H, m, aromatic CH), 8.31 (2H, d, J=8.34 Hz, 1,4-disubstituted benzene), 9.24 (1H, s, CH=N), 12.23 (1H, s, NH). ^{13}C-NMR (75 MHz, DMSO-d_6): δ= 123.05, 124.71, 125.97, 126.04, 127.42, 127.88, 128.16, 130.13, 132.02, 133.65, 134.90, 134.99, 136.37, 139.57, 142.84, 148.46, 149.81, 151.93,

167.14, 168.54. Anal. calcd. For $C_{22}H_{15}N_4O_3Cl$, C, 63.09; H, 3.61; N, 13.38. Found: C, 62.88; H, 3.60; N, 13.41.

3.1.2. Antimicrobial activity

The synthesized ten compounds were investigated for their potential antimicrobial activities against *S. aureus* ATCC 29213, *E. coli* ATCC 25922 (Gram-positive and Gram-negative bacteria, respectively), *C. albicans* ATCC 10231 (fungus), and the clinical isolates of these microorganisms. The study was conducted according to the Clinical Laboratory Standards Institute (CLSI) M100-S28 protocol for bacteria [28], and CLSI M27-A3 protocol for fungi [29]. In the study, Mueller Hinton Broth (MHB) and RPMI-1640 mediums were used for the determination of potential antibacterial and antifungal activity, respectively.

Firstly, all compounds were dissolved in DMSO and the serial dilutions of each compound at the range of 2-512 µg/mL were prepared in 96-well microplates, after placing broth medium in each well. Suspension of each microorganism was prepared using McFarland 0.5 standard and as a result 10^5 CFU/ml densities were reached. Microplates containing bacteria and fungus were incubated for 24 h at 37°C and 48 h at 35°C, respectively. The reference antimicrobials were tested against these microorganisms at the same time. Besides, growth control of microorganisms and sterilization control of the mediums were tested. The wells with the lowest concentration with no microbial growth were determined as minimum inhibition concentrations. The detection was made by visual evaluation using dye MTT [30]. Each test was run thrice.

3.1.3. Anticancer Activity

Cell Culture: HT-29, the colorectal cancer cell line was purchased from American Type Culture Collection and was grown in Dulbecco's modified Eagle's medium (DMEM; Gibco, Thermo Fisher Scientific), supplemented with 10% fetal bovine serum (FBS; Sigma Aldrich), 1% L-glutamine (Sigma-Aldrich), and 1% penicillin/streptomycin (Sigma-Aldrich). The cultured cells were incubated at 37°C in a humidified atmosphere containing 5% CO_2. All newly synthesized compounds were dissolved in DMSO, and stock solutions were diluted with DMEM as the final concentration of DMSO should not exceed 0.5%.

Cell Viability Assay: The effect of the compounds **3a-3j** on the viability of HT-29 cell line was analyzed by MTT assay. The cells were seeded at a density of 1×10^4 cells/well and treated with 20 µM concentrations for each and incubated for 24 h. Untreated cells were used as control and fluorouracil was used for positive control. Following incubation, the cells were treated with 20 μL of MTT solution (5 mg/mL in PBS, Sigma) and incubated at 37°C for 3 h to let the metabolically active cells reduce MTT dye into formazan crystals. The formazan crystals were dissolved in DMSO (Sigma). The reduction of MTT was quantified by measuring the absorbance at 540 nm with a microplate reader (Thermo, Germany). Data was represented as mean ± standard deviation (± SD).

3.1.4. TAS & TOS activity

The total antioxidant status (TAS) was determined by a commercial kit that is manufactured by Rel Assay Diagnostics. According to this method, the potential antioxidant structures in the sample were reduced from the dark blue-green ABTS radical form to the colorless reduced ABTS form. The alteration of absorbance at 660 nm is related to the total antioxidant capacity of the sample. The assay was calibrated with the reference substance used as the stable standard antioxidant solution, which is the vitamin E analogue called the Trolox equivalent. TAS measurement was performed according to the kit procedure. After calculating the difference between absorbance values, the equation given below was calculated according to Eq. 1 [31].

$$A2 - A1 = \Delta Abs\ of\ standart\ or\ sample\ or\ H_20$$
$$Results = \frac{[\Delta Abs\ H_2O - \Delta Abs\ Sample]}{[\Delta Abs\ H_2O - \Delta Abs\ Standart]} \quad (1)$$

Oxidants present in the sample oxidize the ferrous ion-chelator complex to ferric ion. The oxidation reaction is prolonged by enhancer molecules, which are abundantly present in the reaction medium. The ferric ion makes a colored complex with chromogen in an acidic medium. The color intensity, which can be measured spectrophotometrically is related to the total amount of oxidant molecules present in the sample. The assay was calibrated with hydrogen peroxide and the results were expressed in terms of micromolar hydrogen peroxide equivalent per liter (µmol H_2O_2 Equiv./L). TOS measurement was performed according to the kit procedure. After calculating the difference between absorbance values, the equation given below is calculated according to Eq. 2 [32].

$$A2 - A1 = \Delta Abs\ of\ standart\ or\ sample$$
$$Results = \frac{\Delta Abs\ Sample}{\Delta Abs\ Standart} * 20 \quad (2)$$

3.2. Computational details

3.2.1. Density Functional Theory (DFT) calculations

Density functional theory (DFT) was developed by Hohenberg and Kohn [33] and Kohn and Sham [34]. Kohn and Sham reduced the problem of interacting electron systems to the problem of non-interacting electrons moving at an effective potential, which includes the Coulomb interaction between electrons. The most important advantage of this approach is that it can calculate the energy of such a system from the solution of the one-electron Schrödinger equation. Kohn-Sham equations are solved numerically by repeating the so-called self-consistency loop procedure. In each step of this cycle, the energy is calculated and this process continues until it converges to the ground state energy.

In this study, the newly synthesized ten compounds were modeled with DFT by using conventional hybrid functional (B3LYP) [25] and by taking into account long-range interaction (wB97X-D) [26]. Both van der Waals and solvent effect on molecular structure were investigated. All calculations were carried out using Gaussian 09 software [35], and Gauss View 5.0 [36] for visualization. B3LYP functional of Becke, Lee, Yang and Parr was used in comparison to wB97X-D functional which is using a version of Grimme's D2 dispersion model [37]. The two methods were compared in terms of both, energy and geometric parameters and were superimposed by using Olex2 [38] to see the harmony between them. All the calculations were executed both in gas phase and solvent mediums, which are acetonitrile (MeCN), dimethylsulfoxide (DMSO), ethanol (EtOH) and methanol (MeOH) solvents. Polarizable Continuum Model (PCM) [39–42] was used for evaluating the solvent effect on geometry optimization.

According to Koopmans' theorem, the global reactivity parameters were computed, which are electronegativity (χ), chemical potential (μ), hardness (η), electrophilicity index (ω), and softness (S). Chemical reactivity order was determined from the highest-occupied molecular orbital (HOMO) and the lowest-unoccupied molecular orbital (LUMO) analysis.

3.2.2. Theoretical ADMET studies

Computational absorption, distribution, metabolism, excretion, and toxicity properties of compound **3d** with the best antioxidant activity were performed by pkCSM-pharmacokinetics server (http://biosig.unimelb.edu.au/pkcsm/) [43].

3.3. PXRD data analysis

Compound **3a** was characterized with Bruker D8 Advance X-ray diffractometer.

4. Conclusion

A series of some new benzimidazole-hydrazone derivatives (**3a-3j**) was synthesized in this study. The structures of target substances were confirmed by using ^{1}H NMR and ^{13}C NMR spectroscopy and mass spectrometry. The synthesized compounds have been evaluated for antimicrobial activity against four bacterial strains (*S. aureus* and *E. coli*) and two fungal strains (*C. albicans*). The anticancer activities of the compounds were evaluated against the HT-29 cell line. The compounds were also analyzed for their antioxidant capacity by Tas & Tos activity. According to the results, the compounds showed moderate activity against HT-29 cell line. It was determined that the compound **3d** showed a high oxidative effect with 30.81 µmol H_2O_2 Equiv./L value.

Declaration of Competing Interest

There are no conflicts to declare.

CRediT authorship contribution statement

Ayşen IŞIK: Conceptualization, Methodology. **Ulviye Acar Çevik:** Conceptualization, Methodology. **Ismail Çelik:** Visualization. **Hayrani Eren Bostancı:** Methodology, Validation. **Arzu Karayel:** Visualization. **Ufuk Ince:** Methodology. **Ahmet Koçak:** Formal analysis. **Yusuf Özkay:** Formal analysis. **Zafer Asım Kaplancıklı:** Formal analysis.

Acknowledgments

The numerical calculations reported in this paper were partially performed at TUBITAK ULAKBIM, High Performance, and Grid Computing Center (TRUBA resources).

References

[1] C.M. Bagi, Summary-Cancer cell metastasis session, J. Musculoskelet. Neuronal Interact. 2 (2002) 579–580, doi:10.1111/j.1540-6261.1992.tb04673.x.
[2] D.M. Parkin, Global cancer statistics in the year 2000, Lancet Oncol. 2 (2001) 596 -596, doi:10.1016/S1470-2045(01)00486-7.
[3] N. Aydemir, R. Bilaloğlu, Genotoxicity of two anticancer drugs, gemcitabine and topotecan, in mouse bone marrow *in vivo*, Mutat. Res. 537 (2003) 43–51, doi:10.1016/s1383-5718(03)00049-4.
[4] R.M. Klevens, M.A. Morrison, J. Nadle, S. Petit, K. Gershman, S. Ray, Invasive methicillin-resistant Staphylococcus aureus infections in the United States, JAMA 298 (2007) 1763–1771, doi:10.1001/jama.298.15.1763.
[5] S.M. Mousavi, M. Zarei, S.A. Hashemi, A. Babapoor, A.M. Amani, A conceptual review of rhodanine: current applications of antiviral drugs, anticancer and antimicrobial activities, Artif. Cells Nanomed. Biotechnol. 47 (2019) 1132–1148, doi:10.1080/21691401.2019.1573824.
[6] G. Bjelakovic, D. Nikolova, L.L. Gluud, R. Simonetti, G.C. Gand, Mortality in randomized trials of antioxidant supplements for primary and secondary prevention: systematic review and meta-analysis, JAMA 297 (2007) 842–857, doi:10.1001/jama.297.8.842.
[7] H. Sies, Oxidative stress: oxidants and antioxi-dants, Exp. Physiol. 82 (1997) 291–295, doi:10.1113/expphysiol.1997.sp004024.
[8] Z. Liu, B. Wang, Z. Yang, Y. Li, D. Qin, T. Li, Synthesis, crystal structure, DNA interaction and antioxidant activities of two novel water-soluble Cu(2+) complexes derivated from 2-oxoquinoline-3-carbaldehyde Schiff-bases, Eur. J. Med. Chem. 44 (2009) 4477–4484, doi:10.1016/j.ejmech.2009.06.009.
[9] H. Hussain, G. Babic, T. Durst, J. Wright, M. Flueraru, A. Chichirau, L.L. Chepelev, Development of novel antioxidants: design, synthesis, and reactivity, J. Org. Chem. 68 (2003) 7023–7032, doi:10.1021/jo0301090.
[10] T.D. Penning, G.D. Zhu, V.B. Gandhi, J. Gong, X. Liu, Y. Shi, V.L. Giranda, Discovery of the poly (ADP-ribose) polymerase (PARP) inhibitor 2-[(R)-2-methylpyrrolidin-2-yl]-1 H-benzimidazole-4-carboxamide (ABT-888) for the treatment of cancer, J. Med. Chem. 52 (2009) 514–523, doi:10.1021/jm801171j.
[11] A. Romero-Castro, I. León-Rivera, L.C. Ávila-Rojas, G. Navarrete-Vázquez, A. Nieto-Rodríguez, Synthesis and preliminary evaluation of selected 2-aryl-5 (6)-nitro-1 H-benzimidazole derivatives as potential anticancer agents, Arch. Pharm. Res. 34 (2011) 181–189, doi:10.1007/s12272-011-0201-5.
[12] H.T. Abdel-Mohsen, F.A. Ragab, M.M. Ramla, H.I. El Diwani, Novel benzimidazole–pyrimidine conjugates as potent antitumor agents, Eur. J. Med. Chem. 45 (2010) 2336–2344, doi:10.1016/j.ejmech.2010.02.011.
[13] S. Demirayak, U.A. Mohsen, A.Ç. Karaburun, Synthesis and anticancer and anti-HIV testing of some pyrazino [1, 2-a] benzimidazole derivatives, Eur. J. Med. Chem. 37 (2002) 255–260, doi:10.1016/S0223-5234(01)01313-7.
[14] S. Demirayak, I. Kayagil, L. Yurttas, L. Microwave supported synthesis of some novel 1, 3-Diarylpyrazino [1, 2-a] benzimidazole derivatives and investigation of their anticancer activities, Eur. J. Med. Chem. 46 (2011) 411–416, doi:10.1016/j.ejmech.2010.11.007.
[15] S.A. Galal, K.H. Hegab, A.M. Hashem, N.S. Youssef, Synthesis and antitumor activity of novel benzimidazole-5-carboxylic acid derivatives and their transition metal complexes as topoisomerease II inhibitors, Eur. J. Med. Chem. 45 (2010) 5685–5691, doi:10.1016/j.ejmech.2010.09.023.
[16] E. Moriarty, M. Carr, S. Bonham, M.P. Carty, F. Aldabbagh, Synthesis and toxicity towards normal and cancer cell lines of benzimidazolequinones containing fused aromatic rings and 2-aromatic ring substituents, Eur. J. Med. Chem. 45 (2010) 3762–3769, doi:10.1016/j.ejmech.2010.05.025.
[17] B.V.S. Kumar, S.D. Vaidya, R.V. Kumar, S.B. Bhirud, R.B. Mane, Synthesis and anti-bacterial activity of some novel 2-(6-fluorochroman-2-yl)-1-alkyl/acyl/aroyl-1H-benzimidazoles, Eur. J. Med. Chem. 41 (2010) 599–604, doi:10.1016/j.ejmech.2006.01.006.
[18] G.A. Kilcigil, N. Altanlar, Synthesis and antifungal properties of some benzimidazole derivatives, Turk. J. Chem. 30 (2006) 223–228.
[19] I. Kerimov, G. Ayhan-Kilcigil, B. Can-Eke, N. Altanlar, M. İscan, Synthesis, antifungal and antioxidant screening of some novel benzimidazole derivatives, J. Enzyme Inhib. Med. Chem. 22 (2007) 696–701, doi:10.1080/14756360701228558.
[20] D. Sharma, B. Narasimhan, P. Kumar, V. Judge, R. Narang, E. De Clercq, J. Balzarini, Synthesis, antimicrobial and antiviral activity of substituted benzimidazoles, J. Enzyme Inhib. Med. Chem. 24 (2009) 1161–1168, doi:10.1080/14756360802694427.
[21] R.K. Mohapatra, A.K. Sarangi, M. Azam, M.M. El-ajaily, M. Kudrat-E-Zahan, S.B. Patjoshi, D.C. Dash, Synthesis, structural investigations, DFT, molecular docking and antifungal studies of transition metal complexes with benzothiazole based Schiff base ligands, J. Mol. Struct. 1179 (2019) 65–75, doi:10.1016/j.molstruc.2018.10.070.
[22] C. Kus, G. Ayhan-Kilcigil, B.C. Eke, Synthesis and antioxidant properties of some novel benzimidazole derivatives on lipid peroxidation in the rat liver, Arch. Pharm. Res. 27 (2004) 156–163, doi:10.1007/bf02980099.
[23] C. Kuş, G. Ayhan-Kılcıgil, S. Özbey, F.B. Kaynak, M. Kaya, T. Çoban, B. Can-Eke, Synthesis and antioxidant properties of novel N-methyl-1, 3, 4-thiadiazol-2-amine and 4-methyl-2H-1, 2, 4-triazole-3 (4H)-thione derivatives of benzimidazole class, Bioorg. Med. Chem. 16 (2008) 4294–4303, doi:10.1016/j.bmc.2008.02.077.
[24] R.K. Mohapatra, M.M. El-ajaily, F.S. Alassbaly, A.K. Sarangi, D. Das, A.A. Maihub, S.F. Ben-Gweirif, A. Mahal, M. Suleiman, L. Perekhoda, M. Azam, T.H. Al-Noor, DFT, anticancer, antioxidant and molecular docking investigations of some ternary Ni (II) complexes with 2-[(E)-[4-(dimethylamino) phenyl] methyleneamino] phenol, Chem. Pap. 75 (2021) 1005–1019, doi:10.1007/s11696-020-01342-8.
[25] B.S. Lee, Causal relations among stock returns, interest rates, real activity, and inflation, J. Finance. 47 (1992) 1591–1603, doi:10.1111/j.1540-6261.1992.tb04673.x.
[26] Y.S. Lin, G.D. Li, S.P. Mao, J.D. Chai, Long-range corrected hybrid density functionals with improved dispersion corrections, J. Chem. Theory Comput. 9 (2013) 263–272, doi:10.1021/ct300715s.
[27] U. Acar Çevik, B.N. Sağlık, D. Osmaniye, S. Levent, B. Kaya Çavuşoğlu, A.B. Karaduman, Z.A. Kaplancıklı, Synthesis, anticancer evaluation and molecular docking studies of new benzimidazole-1, 3, 4-oxadiazole derivatives as human topoisomerase types I poison, J. Enzyme Inhib. Med. Chem. 35 (2020) 1657–1673, doi:10.1080/14756366.2020.1806831.
[28] A.M. Bobenchik, E. Deak, J.A. Hindler, C.L. Charlton, R.M. Humphries, Performance of Vitek 2 for antimicrobial susceptibility testing of acinetobacter baumannii, Pseudomonas aeruginosa, and Stenotrophomonas maltophilia with Vitek 2 (2009 FDA) and CLSI M100S 26th Edition Breakpoints, J. Clin. Microbiol. 55 (2017) 450–456, doi:10.1128/jcm.01859-16.
[29] P. Wayne. Clinical and laboratory standards institute: reference method for broth dilution antifungal susceptibility testing of yeasts; approved standard. CLSI document M27-A3. 3 (2008) 6-12.
[30] L. Shi, H.M. Ge, S.H. Tan, H.Q. Li, Y.C. Song, H.L. Zhu, R.X. Tan, Synthesis and antimicrobial activities of Schiff bases derived from 5-chloro-salicylaldehyde, Eur. J. Med. Chem. 42 (2007) 558–564, doi:10.1016/j.ejmech.2006.11.010.
[31] O. Erel, A novel automated direct measurement method for total antioxidant capacity using a new generation, more stable ABTS radical cation, Clin. Biochem. 37 (2004) 277–285, doi:10.1016/j.clinbiochem.2003.11.015.
[32] O. Erel, A new automated colorimetric method for measuring total oxidant status, Clin. Biochem. 38 (2005) 1103–1111, doi:10.1016/j.clinbiochem.2005.08.008.
[33] P. Hohenberg, W. Kohn, Inhomogeneous electron gas, Phys. Rev. 136 (1964) B864.

[34] W. Kohn, L.J. Sham, Self-consistent equations including exchange and correlation effects, Phys. Rev. 140 (1965) A1133.
[35] M.J. Frisch, W.G. Trucks, H.B. Schlegel, G.E. Scuseria, M.A. Robb, J.R. Cheeseman, G. Scalmani, V. Barone, B. Mennucci, G.A. Petersson, H. Nakatsuji, M. Caricato, X. Li, H.P. Hratchian, A.F. Izmaylov, J. Bloino, G. Zheng, J.L. Sonnenberg, M. Hada, M. Ehara, K. Toyota, R. Fukuda, J. Hasegawa, M. Ishida, T. Nakajima, Y. Honda, O. Kitao, H. Nakai, T. Vreven, J.A. Montgomery, J.E. Peralta, F. Ogliaro, M. Bearpark, J.J. Heyd, E. Brothers, K.N. Kudin, V.N. Staroverov, T. Keith, R. Kobayashi, J. Normand, K. Raghavachari, A. Rendell, J.C. Burant, S.S. Iyengar, J. Tomasi, M. Cossi, N. Rega, J.M. Millam, M. Klene, J.E. Knox, J.B. Cross, V. Bakken, C. Adamo, J. Jaramillo, R. Gomperts, R.E. Stratmann, O. Yazyev, A.J. Austin, R. Cammi, C. Pomelli, J.W. Ochterski, R.L. Martin, K. Morokuma, V.G. Zakrzewski, G.A. Voth, P. Salvador, J.J. Dannenberg, S. Dapprich, A.D. Daniels, O. Farkas, J.B. Foresman, J.V. Ortiz, J. Cioslowski, D.J. Fox, Gaussian 09. Revision C.01, Gaussian, Inc., Wallingford CT, 2010.
[36] D. Roy, K. Todd, M. John, GaussView. Version 5, Semichem Inc., Shawnee Mission, KS, 2009.
[37] S. Grimme, Semiempirical hybrid density functional with perturbative second-order correlation, J. Chem. Phys. 124 (2006) 034108, doi:10.1063/1.2148954.
[38] O.V. Dolomanov, L.J. Bourhis, R.J. Gildea, J.A.K Howard, H. Puschmann, Olex2-1.2 program. A complete structure solution, refinement and analysis program, J. Appl. Crystallogr. 42 (2009) 339–340, doi:10.1063/1.2148954.
[39] E. Cancès, B. Mennucci, J. Tomasi, A new integral equation formalism for the polarizable continuum model: theoretical background and applications to isotropic and anisotropic dielectrics, J. Chem. Phys. 107 (1997) 3032–3041, doi:10.1063/1.474659.
[40] B. Mennucc, J. Tomasi, Continuum solvation models: a new approach to the problem of solute's charge distribution and cavity boundaries, J. Chem. Phys. 106 (1997) 5151–5158, doi:10.1063/1.473558.
[41] B. Mennucci, E. Cancès, J. Tomasi, Evaluation of solvent effects in isotropic and anisotropic dielectrics and in ionic solutions with a unified integral equation method: theoretical bases, computational implementation, and numerical applications, J. Phys. Chem. B 101 (1997) 10506–10517, doi:10.1021/jp971959k.
[42] J. Tomasi, B. Mennucci, E. Cancès, The IEF version of the PCM solvation method: an overview of a new method addressed to study molecular solutes at the QM ab initio level, J. Mol. Struct. Theochem. 464 (1999) 211–226, doi:10.1016/S0166-1280(98)00553-3.
[43] D.E. Pires, T.L. Blundell, D.B. Ascher, pkCSM: predicting small-molecule pharmacokinetic and toxicity properties using graph-based signatures, J. Med. Chem. 58 (2015) (2015) 4066–4072, doi:10.1021/acs.jmedchem.5b00104.
[44] A.A. Coelho, (2012). TOPAS Academic Version 5: User Manual.